

Published in final edited form as:

*Int J Immunopathol Pharmacol.* 2005 ; 18(3): 391–402.

## MACROPHAGE-TARGETED PHOTODYNAMIC THERAPY: SCAVENGER RECEPTOR EXPRESSION AND ACTIVATION STATE

Q. LIU<sup>1,2</sup> and M. R. HAMBLIN<sup>1,2,3</sup>

<sup>1</sup>Wellman Center for Photomedicine, Massachusetts General Hospital, Boston, MA

<sup>2</sup>Department of Dermatology, Harvard Medical School, Boston, MA

<sup>3</sup>Harvard-MIT Division of Health Sciences and Technology, Cambridge, MA, USA

### Abstract

Macrophage-targeted photodynamic therapy (PDT) may have applications in the selective killing of cells involved in atherosclerosis, inflammation and tumor. We have previously shown that a conjugate between the photosensitizer chlorin(e6) (ce6) and maleylated bovine serum albumin (BSA-mal) gives highly selective targeting to macrophages. In this report we examine the effect of macrophage activation and scavenger receptor class A (SRA) expression on this targeting in two murine macrophage tumor cell lines (RAW264.7 and P388D1) and a control murine mammary sarcoma cell line (EMT-6). Cells were pretreated with interferon gamma (IFN $\gamma$ ) and/or lipopolysaccharide (LPS) followed by BSA-ce6-mal addition, and SRA expression, tumor necrosis factor alpha (TNF $\alpha$ ) release, conjugate uptake and PDT killing were measured. Both macrophage cell lines expressed SRA and took up conjugate specifically in an SRA-dependent manner, but differences were observed in their response to activation. RAW264.7 expressed increasingly more SRA and took up increasingly more BSA-ce6-mal in response to IFN $\gamma$ , LPS, and IFN $\gamma$ +LPS, respectively. The PDT killing did not follow the same pattern as the uptake of the photosensitizer. The increase in uptake in the IFN $\gamma$  treated cells did not lead to an increase in PDT killing, while stimulation with LPS or IFN $\gamma$ +LPS resulted in a significant protection against PDT, despite a significant increase in photosensitizer uptake. P388D1 was responsive to neither IFN $\gamma$ , nor to LPS, or to IFN $\gamma$ +LPS with respect to SRA expression, conjugate uptake, and PDT killing. These data may have implications for the use of PDT to target physiologically undesirable macrophage subtypes implicated in disease, and on how manipulation of the activation status of the macrophage will influence the PDT effect.

### Keywords

photodynamic therapy; macrophages; scavenger receptor; photosensitizer conjugate; interferon gamma; lipopolysaccharide; tumor necrosis factor alpha

---

Although macrophages are important cells for homeostasis and immunity, they are also involved in many human diseases. They play a pivotal role both in the development of atherosclerosis (1), and also in the vulnerability of the atherosclerotic plaques to rupture (2), an occurrence that frequently precipitates heart attacks (3). Macrophages are involved in the

---

Copyright © by BIOLIFE, s.a.s.

Mailing address: Dr Michael R. Hamblin, BAR414, Wellman Center for Photomedicine, Massachusetts General Hospital, 40 Blossom Street, Boston MA 02114. Tel: 617-726-6182; Fax: 617-726-8566, hamblin@helix.mgh.harvard.edu.

pathology arising from many infectious and inflammatory diseases and have been implicated in the progression of some cancers (4). They therefore represent a prime target for therapeutic intervention (5). However, it is obvious that only the macrophages that are involved in the disease that is undesirable, while the majority of monocyte-macrophages in the circulation and in healthy tissues are valuable and productive cells. Hence, although it is possible in principle to administer selective macrophage toxins that would kill all cells of the monocyte-macrophage lineage, this would be unnecessarily severe and uncertain (6). A method of killing only those macrophages in a certain anatomical location implicated in disease would be desirable. This goal may be accomplished using macrophage-targeted photodynamic therapy (PDT). In PDT a non-toxic dye termed a photosensitizer (PS) that is taken up by a cell is activated with low intensity visible light and in the presence of oxygen forms reactive oxygen species capable of causing cell death (frequently by apoptosis) (7). In recent years workers have targeted PS to cancer cells via monoclonal antibodies that recognize tumor-associated antigens (8-9), and to bacteria via polycationic polymers (10). By covalently attaching the PS to a macromolecule that is specifically recognized by cell surface receptors expressed on macrophages, and by only illuminating the diseased tissue, targeted destruction of macrophages may be achieved (11).

We have previously described (12) a system whereby this goal is accomplished by covalently attaching the PS ce6 to maleylated serum albumin (BSA-mal), a classic ligand of the class A scavenger receptor (SRA). However, whether this macrophage specific accumulation of the ce6 and BSA-mal conjugate (BSA-ce6-mal) is still SRA-dependent is unknown. SRA expression is largely confined to mature macrophages (13). The PS-conjugate was taken up by the murine macrophage cell line (J774A1) by receptor-mediated endocytosis, and was accumulated in lysosomes. Very selective phototoxicity of target cells was achieved, while non-macrophage cells were left unharmed. In order to further define the utility of this methodology we have extended the study in the present report to two other murine macrophage cell lines (RAW264.7 and P388D1).

Macrophages are activated by many inter-related pathways, of which in many cases are consequences of their primary functions as the cell type responsible for orchestrating innate immunity (14). This response to pathogenic microorganisms involves initial pattern recognition of structures (lipopolysaccharide (LPS), teichoic acid, bacterial DNA, beta-glucan, etc.) peculiar to microbes (15). The recognition is carried out by receptors such as Toll-like receptors (16), CD14 (17), and beta-glucan receptor (18), that activate signaling pathways leading to expression of a wide variety of genes such as tumor-necrosis factor alpha (TNF $\alpha$ ), interleukins and inducible nitric oxide synthase (19). Interferon gamma (IFN $\gamma$ ) is known to prime macrophages to respond to these microbial stimuli (20). Since macrophages responsible for causing disease tend to be in an activated state, we asked how effective is scavenger-receptor mediated PDT in killing activated macrophages. We therefore examined the SRA-dependency and effect of the classical activation pathway (IFN-g and/or LPS) on the uptake of BSA-ce6-mal and consequent phototoxicity of the scavenger-receptor targeted PS-conjugate.

## MATERIALS AND METHODS

### Cell lines

Mouse macrophage-like cell lines, RAW264.7, and P388D1, and mammary sarcoma cell line EMT6, were all obtained from ATCC (Rockville, MD). Cells were grown in RPMI 1640 media containing HEPES, glutamine, 10% fetal calf serum (FCS, Hyclone, Logan, VT), 100 U/ml penicillin and 100  $\mu$ g/ml streptomycin. The endotoxin levels were measured in the final complete medium with an LAL test kit (Cape Code Associates, Falmouth, MA) and were all below 0.1 U/ml.

### Preparation of BSA-c<sub>e6</sub>-mal conjugate

This was carried out as previously described (12). In brief, low endotoxin BSA (Sigma Chemical Co, St Louis, MO) was reacted with the preformed N-hydroxy succinimide ester of c<sub>e6</sub> in NaHCO<sub>3</sub> buffer (0.1 M, pH 9.3) and, after standing in the dark at room temp for 6 hours, the BSA-c<sub>e6</sub> was maleylated by adding solid maleic anhydride in portions to the protein preparation with vortex mixing and addition of saturated NaHCO<sub>3</sub> solution as needed to keep the pH above 7 (21). The reaction mixture was allowed to stand at room temp in the dark for 3 hours. The crude BSA-c<sub>e6</sub>-mal was purified by repeated acetone precipitation followed by exhaustive dialysis. BSA-c<sub>e6</sub>-mal preparations were checked for endotoxin content by Limulus amoebocyte assay (Associates of Cape Cod Inc, Falmouth, MA) and the value was less than 0.2 Units/ml when the conjugate was used at 2 μM c<sub>e6</sub> equivalent.

### Macrophage activation

Cells were grown in complete medium at a density of 10,000 per well of a 24-well plate. Fresh medium containing 100 units/mL murine IFN $\gamma$  (Peprotech Rocky Hill, NJ) was added and the cells incubated for 48 hours. In a similar fashion fresh medium containing from 1 ng/mL to 5 μg/mL LPS from *Salmonella typhimurium* (Sigma) was added to cells which were incubated for 24 hours. In the case of dual stimulation IFN $\gamma$  was added for 24 hours and LPS added to the IFN $\gamma$  containing medium for a further 24 hours.

### TNF $\alpha$ determination

TNF $\alpha$  concentration in cell culture was measured using a cytometric bead array (Pharmingen, San Diego, CA) following the manufacturer's instructions. Briefly, 5 sets of polymer beads each conjugated with distinct known levels of marker fluorescence in the fluorescence channel 3, and each set conjugated with an antibody against a different analyte (anti-TNF $\alpha$ , anti-IFN $\gamma$ , anti-IL2, anti-IL4, anti-IL5) were mixed with the sample to be measured. Then a detection reagent was added and the reaction mixture was incubated at room temperature in the dark for 2 hours, as instructed. The beads were washed and bead-associated fluorescence was read on a FACScalibur (BD Bioscience, San Jose, CA). The marker fluorescence was used to identify the set of beads to which a known antibody was attached, and the reporting fluorescence in fluorescence channel 2 was obtained on the gated beads. This reporting fluorescence represents the signal from the binding of the analyte that corresponds to the specificity of the antibody. A standard curve for each analyte was obtained and the concentration of each analyte was calculated. Five cytokines (TNF $\alpha$ , IFN $\gamma$ , IL-2, IL-4, and IL-5) were measured simultaneously in one single sample, however in this study only TNF $\alpha$  was of any interest.

### Scavenger receptor expression

Cells were removed from the plates incubating with a non-enzymatic dissociation reagent (Sigma, St. Louis, MO). Cells were washed and resuspended in PBS containing 0.1% BSA. 100 μl of cell suspension was then incubated on ice with FITC labeled anti-SR antibody (2F8), or isotype-matched control IgG2b (both from Accurate Corp., Westbury, NY) at a final concentration of 20 nM for 2 hours. The incubation mixture was then diluted with 2ml buffer washed. Cells were then resuspended in 200 μl PBS containing 0.1% BSA and cell-associated fluorescence was determined by flow cytometry.

### Uptake of BSA-c<sub>e6</sub>-mal

Cells were washed with PBS 2 times, and complete RPMI 1640 medium containing different concentrations of BSA-c<sub>e6</sub>-mal were added and incubated for 24 hours. Then cells were removed by incubation with PBS containing 2 mM EDTA and pipetting (RAW264.7

and P388D1) or by trypsin (for EMT6), and washed with PBS and cell-associated fluorescence was determined by flow cytometry. Fluorescence was excited by 488-nm laser and forward scatter and side scatter were set to E-01 and 250 respectively. A 670-nm long pass filter in FL3 channel allowed  $c_{e6}$  fluorescence to be measured with a photomultiplier tube setting of 600. In some experiments the cells were preincubated with unlabeled 2F8 antibody at a concentration of 20 nM for 1 hour before addition of the BSA- $c_{e6}$ -mal.

### Confocal Microscopy

Cells grown on coverslips were incubated with 2  $\mu$ M of BSA- $c_{e6}$ -mal conjugate for 24 hours. Then the cells were washed with PBS and the coverslip was laid inverted on a drop of aqueous immersion fluid on a glass slide. The red intracellular fluorescence from  $c_{e6}$  was imaged in the cells using a Leica DMR confocal laser fluorescence microscope (Leica Mikroskopie und Systeme GmbH, Wetzlar, Germany) (excitation 488 nm argon laser) and a 100X oil immersion objective was used to image at a resolution of 1024  $\times$  1024 pixels. Fluorescence signals in the red range (580 nm dichroic mirror plus 590 nm longpass filter) and phase contrast images captured using TCS NT software (Version 1.6.551, Leica Lasertechnik, Heidelberg, Germany).

### PDT studies

Cells were seeded in flat-bottomed polystyrene 96 well plates (Nunc, Rochester, NY). Because different cells treated with different stimulating conditions (IFN $\gamma$  and/or LPS) grow at different rates, seeding densities were adjusted that the readings of OD<sub>540</sub> from the MTT assay for the non-illuminated wells for all the treatments were all comparable. After activation (or not) and incubation with BSA- $c_{e6}$ -mal, cells were washed 2 times with PBS and 100  $\mu$ l PBS were added to each well. Then cells were illuminated from below with a spot generated by a 670-nm diode laser via a fiber optic coupled microscope objective at a fluence rate of 50 mW/cm<sup>2</sup>. Fluences delivered were 0.5, 1, 2, 5, and 10 J/cm<sup>2</sup>. After illumination, PBS was replaced with complete RPMI 1640 medium and cells were incubated for 24 hours. Cell survival was determined by the 3-(4,5-dimethylthiazol-2-yl)-2,5-diphenyltetrazolium bromide (MTT) assay, which measures mitochondrial dehydrogenase activity. It has been extensively used for measuring viability of cell cultures after PDT and has been shown to have a close correlation with colony forming assays (22). 10  $\mu$ l MTT solution of 5 mg/mL was then added to each well and incubated under 5% CO<sub>2</sub> at 37°C for 4 hours. The medium was then carefully removed and 50  $\mu$ l of dimethyl sulfoxide was added. Plates were gently shaken on an orbital shaker in the dark for 15 min to complete the dissolution of formazan crystals and the absorbances of the samples were read on a plate reader (Model 2550 EIA, Bio-Rad Laboratories, Hercules, CA) at 540 nm. Cells survival fractions were calculated as ratios of OD<sub>540</sub> to that of nonilluminated samples incubated with conjugate.

### Statistics

Unpaired 2-tailed student's *t*-test assuming equal or unequal variation in the standard deviation as appropriate was used to compare the means between different groups.  $P < 0.05$  was considered significant. \* =  $P < 0.05$ ; \*\* =  $P < 0.01$ ; \*\*\* =  $P < 0.001$ .

## RESULTS

### Macrophage activation

Both RAW264.7 and P388D1 cells secrete a measurable base level of TNF $\alpha$ . In response to IFN $\gamma$ , RAW264.7 dramatically increases its RAW264.7 secretion (4 fold). LPS induces even high TNF $\alpha$  production (6 fold). IFN $\gamma$ +LPS increases the TNF $\alpha$  secretion to the same level as

IFN $\gamma$  alone. With P388D1 cells, IFN $\gamma$  or LPS alone has minimal effect, even IFN $\gamma$ +LPS induces only a 2-fold increase. Addition of the BSA-ce6-mal conjugate at concentrations used for PDT experiments does not stimulate any TNF $\alpha$  secretion, demonstrating that the endotoxin level in the conjugate is not influencing the activation status of the cells. As expected the control cell line EMT6 had very low levels of TNF $\alpha$  that were not increased by any of the stimulations.

### Scavenger receptor expression

SRA expression was quantified by surface binding of FITC-labeled antibody 2F8 measured by FACS after incubation of the cells at 4°C to prevent internalization. The results are presented in Figure 2. RAW264.7 cells have a low level SRA expression in the unstimulated state and this is increased after IFN $\gamma$  treatment, further increased by LPS and even further increased by the combination of IFN $\gamma$  and LPS. P388D1 cells have a higher basal level of SRA expression than RAW264.7 cells but this is not altered by any of the stimulations. There was no detectable binding of SRA antibody in excess of isotype matched control IgG on EMT6 cells under any conditions.

### Cellular uptake of conjugate

Ce6 uptake was measured in cells by FACS analysis after incubation with BSA-ce6-mal conjugate (0-5 $\mu$ M ce6 equivalent) in serum-containing medium for 24 h. A histogram of the fluorescence measured in the FL3 channel (670-nm long pass filter) obtained with unstimulated RAW264.7 cells incubated with increasing concentrations of conjugate is shown in Fig. 3. Mean fluorescence intensity for each cell under different conditions at each concentration was obtained from a histogram of 10,000 cells. The complete uptake results are presented in Figures 4a-4c showing mean  $\pm$  SE. RAW264.7 cells showed the same pattern as its SRA expression: IFN $\gamma$ , LPS, and IFN $\gamma$  + LPS stimulated an increasingly higher uptake (Fig. 4a). The lowest uptake was observed with the unstimulated cells, while IFN $\gamma$  alone gave a significantly higher uptake, and both LPS alone and IFN $\gamma$  + LPS gave uptakes that were significantly higher than the other conditions (but not significantly different from each other). P388D1 cells had the same base level uptake as unstimulated RAW264.7 cells, and the uptake was not altered under any of the stimulation conditions (Fig. 4b), consistent with its SRA expression pattern. The control cell line EMT6 gave the lowest uptake, which again was not changed by any of stimulation conditions (Fig. 4c).

### Confocal microscopy

The localization of the red ce6 fluorescence delivered into macrophages was visualized. We previously showed that for unstimulated J774 cells incubated with BSA-ce6-mal the ce6 was predominantly localized in lysosomes. We now asked whether the stimulation of cells by IFN $\gamma$  and/or LPS affected the subcellular localization. Fig 5 a-d shows the phase-contrast photomicrographs together with the fluorescence images obtained for RAW264.7 cells in the unstimulated state and after stimulation with IFN $\gamma$  + LPS. RAW264.7 cells respond to IFN $\gamma$ +LPS with dramatic shape change, from round cells to long fibroblast like shaped. The pattern of ce6 fluorescence also changed dramatically: ce6 appears as clusters of small aggregates in unstimulated cells, while all the fluorescence is in one big clump in cells stimulated with IFN $\gamma$ +LPS. The same change was also observed with another macrophage cell line, the J774 (data not shown). In P388D1 cells, all the ce6 fluorescence is distributed in a horse-shoe shape of small aggregates, regardless of stimulations (data not shown). There is no detectable fluorescence with in the EMT6 cells (data not shown).



### Pre-treatment with blocking antibody

Cells were pre-treated with either the anti-SR antibody 2F8 or isotype matched control IgG2b followed by conjugate addition in order to test how much of the conjugate uptake could be inhibited by blocking of the SR. As can be seen in Fig. 6 the specific uptake of conjugate by RAW264.7 cells and P388D1 cells was reduced by >90%, taking EMT6 as background. The isotype-matched control antibody did not lead to any significant reduction in uptake in any cells, neither did either antibody in EMT6 cells.

### Phototoxicity

Phototoxicity assays were carried out by using the MTT microculture plate technique 24 hours after illumination. Cells were incubated with conjugate for 24 h and then washed, exposed to varying fluences of 670-nm light. The results are presented in Figs 7a-7c. Stimulation of RAW264.7 cells with either LPS or IFN $\gamma$ +LPS significantly reduced PDT killing (Fig. 7a), despite a significant increase in uptake of the photosensitizer conjugate (Fig. 4a). IFN $\gamma$  stimulation did not alter the PDT killing, although it increased the conjugate uptake (Figs 4a and 7a). There was no significant difference in the PDT killings between any of the P388D1 cells (Fig. 7b), which is in good agreement with there being no difference in uptake either (Fig. 4b). As expected the EMT6 cells are not killed at all (Fig. 7c).

We also tested whether illumination of cells that had been pre-incubated with anti-SRA antibody before being incubated with conjugate would be killed. As can be seen in Fig 8, anti-SRA significantly protected both RAW264.7 and P388D1 cells from PDT killing: With RAW264.7 cells, less than 20% killing was observed at light dose of 5 J/cm<sup>2</sup>, comparing to >90% with no antibody control or isotype antibody treated cells (Fig. 8a). With P388D1 cells, a complete protection was achieved: there was virtually no PDT killing in anti-SRA treated cells, while control cells and isotype antibody treated cells were almost killed completely (Fig. 8b). The PDT killings were highly consistent with the corresponding conjugate uptake (Fig. 6).

## DISCUSSION

Because of the importance of macrophages and SRAs in the pathophysiology of atherosclerosis many workers have studied how SRA expression and activity varies between monocyte/macrophages in various states (23-24). The SRA is a multidomain trimeric transmembrane protein expressed by mature macrophages but not monocytes. The precise structural motifs which lead to SRA recognition of ligands are complex and incompletely understood and their function has been referred to as “molecular flypaper” (25). However all ligands appear to be macromolecules that include a polyanionic structure typified by maleylated albumin (21,26). After initial binding, the ligands are rapidly internalized and are routed to lysosomes for degradation by proteases and other lysosomal enzymes. Some of the natural function of SRA that have been reported include: phagocytosis of bacteria and other pathogens, phagocytosis of apoptotic cells, phagocytosis of senescent red blood cells, endocytosis of oxidized low density lipoprotein and advanced glycation end product modified proteins, and calcium independent adhesion (27). Because of the high capacity of SRA to internalize ligands investigators have explored the possibility of preparing covalent conjugates between SRA ligands and various drugs to produce macrophage targeted therapy (12,28). However, the effect of various macrophage activation stimuli on SRA-mediated targeting has not to our knowledge been reported.

In this report we studied the effect of different stimulations on the uptake of the photosensitizer conjugate, BSA-ce6-mal, in two mouse macrophage cell lines, RAW264.7

and P388D1, and a non-macrophage control cell line, the mammary sarcoma cell line, EMT6. The responses to different stimulations were different in different cell lines and also different depending on the parameters measured in the same cell line. RAW264.7 cells express increasingly higher levels of SRA in response to IFN $\gamma$ , LPS, and IFN $\gamma$ +LPS (Fig. 2). Their TNF $\alpha$  secretion increased dramatically with the stimulation of either IFN $\gamma$  or LPS, however, unexpectedly, the combination of the two only led to the same level as IFN $\gamma$  alone and even lower than LPS alone (Fig. 1). This phenomenon was consistently observed. The P388D1 cells responded to either IFN $\gamma$  or LPS alone minimally, and IFN $\gamma$  + LPS although induced a significant increase in TNF $\alpha$  secretion, is much less dramatic comparing to the increase in RAW264.7 cells (Fig. 1). P388D1 cells did not respond at all to either IFN $\gamma$  or LPS or IFN $\gamma$  + LPS in their SRA expression (Fig. 2). This result is in agreement with reports in the literature that describe a mutation in the signal-transduction machinery of P388D1 cells that make them tolerant to LPS (29). This may involve differences in the DNA-binding motif of the TNF $\alpha$  promoter (30), or lack of phosphorylation of I $\kappa$ B $\alpha$  (31).

Not surprisingly, the uptake of the BSA-ce6-mal depends on the level of the SRA expression, unrelated to TNF $\alpha$  secretion: In RAW264.7 cells, IFN $\gamma$ , LPS, and IFN $\gamma$  + LPS induced an increasingly higher uptake (Fig 4a), parallel to their effects on SRA expression (Fig. 2). In P388D1 cells, none of the stimulations showed an effect on SRA expression (Fig. 2), nor did they have an effect on the uptake of the BSA-ce6-mal conjugate (Fig. 4b). However, the increased uptake of the conjugate in RAW264.7 cells did not lead to an increased PDT killing, but instead, those cells showed an increased resistance to PDT (Fig. 7). We consider the following factors that are likely responsible for this discrepancy between conjugate uptake and PDT killing in RAW264.7 cells: First, activation with LPS or IFN $\gamma$ +LPS may lead to upregulation of antioxidant in macrophages as a form of self-protection against the reactive oxygen species generated by activated macrophage cells (32). This could then lead to a reduced sensitivity to the reactive oxygen species generated by PDT. This finding is in agreement with the results of Hunt et al (33) who studied mouse peritoneal macrophages with PDT mediated by benzoporphyrin derivative. They found that IFN $\gamma$  gave similar uptake of PS but more killing, while LPS led to a higher PS uptake but less killing. Another explanation could be the observation of Orlofsky et al (34) that an anti-apoptotic protein A1 (a member of the bcl2 family) is rapidly induced in mouse macrophages (peritoneal and J774 cells) by LPS and protects the cells from death caused by nitric oxide (35). Furthermore, after activation by LPS and IFN $\gamma$ +LPS, the BSA-ce6-mal conjugate forms big clumps within the cell, while they are in small clusters in nonstimulated cells. This clumping of the photosensitizer conjugate is likely to reduce PDT effect via affecting either the absorption of light or the diffusion of the reactive oxygen species to their target, or both.

There have been literature reports concerning an inter-species difference as to the effect LPS has on macrophage scavenger expression. Human monocyte macrophages derived from peripheral blood responded to LPS by reducing the activity of the scavenger receptor as measured by malondialdehyde-modified low-density lipoprotein degradation (36). This reduction in response was also found in macrophages differentiated from the THP1 human monocyte cell line (37). By contrast both J774 and RAW264.7 cells were reported to increase SRA at both mRNA and protein levels in response to LPS (37), but activity was not measured. There are conflicting reports in the literature on the effect of IFN $\gamma$  on human macrophage SRA expression. Geng et al (38) showed that IFN $\gamma$  reduced the number of SRA on the cell surface of human peripheral blood derived macrophages and the activity was also reduced. However Grewal et al (39) showed that less differentiated human monocyte/macrophage cells upregulated SRA after IFN $\gamma$  treatment as judged by mRNA and activity. In our studies IFN $\gamma$  and LPS caused an increase in both SRA surface expression (Fig. 2) and uptake of BSA-ce6-mal (Fig. 4a) in mouse macrophage cell line RAW264.7.

It has been shown that the same ligand with different degree of modification such as heavily oxidized LDL vs mildly oxidized LDL (40), or the same ligand with different modifications such as oxidation vs chlorination or nitration of LDL, resulted in the recognition by different scavenger receptors (SRA vs CD36) (41-43). Although BSA-mal is reported to be an SRA-specific ligand (26,44), and conjugation of ce6 to BSA-mal still leads to macrophage-specific accumulation of the BSA-ce6-mal conjugate and macrophage-specific killing by PDT (12) whether this is also SRA specific is unknown. In this current study we showed that the uptake of BSA-ce6-mal conjugate by mouse macrophage tumor cells is also SRA-specific: monoclonal anti-SRA inhibited the uptake by more than 90% (Fig 6). The inhibition in uptake of BSA-ce6-mal by the anti-SRA antibody resulted in a corresponding protection in PDT killing, as expected (Fig 8).

In conclusion, we found that BSA-ce6-mal induces SRA-dependent selective PDT killing of macrophages. LPS stimulation of macrophages leads to decreased PDT killing despite an increase in conjugate uptake. These types of studies will be necessary if the PDT-mediated destruction of unwanted macrophages is advanced to clinical practice.

## Acknowledgments

This work was funded by the National Institutes of Health, grant number: R01-CA/AI838801.

## REFERENCES

1. Parthasarathy S, Steinberg D, Witztum JL. The role of oxidized low-density lipoproteins in the pathogenesis of atherosclerosis. *Annu. Rev. Med.* 1992; 43:219. [PubMed: 1580586]
2. Cassells W, Hathorn B, David M, Krabach T, Vaughn WK, McAllister HA, Bearman G, Willerson JT. Thermal detection of cellular infiltrates in living atherosclerotic plaques: possible implications for plaque rupture and thrombosis. *Lancet.* 1996; 347:1447. [PubMed: 8676628]
3. Falk E. Why do plaques rupture? *Circulation.* 1992; 86:III30. [PubMed: 1424049]
4. Mantovani A. Tumor-associated macrophages in neoplastic progression: a paradigm for the in vivo function of chemokines. *Lab. Invest.* 1994; 71:5. [PubMed: 7518882]
5. Wahl LM, Kleinman HK. Tumor-associated macrophages as targets for cancer therapy. *J. Natl. Cancer Inst.* 1998; 90:1583. [PubMed: 9811301]
6. Van Rooijen N. The liposome-mediated macrophage 'suicide' technique. *J. Immunol. Meth.* 1989; 124:1.
7. Dougherty TJ, Gomer CJ, Henderson BW, Jori G, Kessel D, Korbek M, Moan J, Peng Q. Photodynamic therapy. *J. Natl. Cancer Inst.* 1998; 90:889. [PubMed: 9637138]
8. Molpus KL, Hamblin MR, Rizvi I, Hasan T. Intraperitoneal photoimmunotherapy of ovarian carcinoma xenografts in nude mice using charged photoimmunoconjugates. *Gynecol. Oncol.* 2000; 76:397. [PubMed: 10684717]
9. Hamblin MR, Governatore MD, Rizvi I, Hasan T. Biodistribution of charged 17.1A photoimmunoconjugates in a murine model of hepatic metastasis of colorectal cancer. *Br. J. Cancer.* 2000; 83:1544. [PubMed: 11076666]
10. Demidova TN, Hamblin MR. Photodynamic therapy targeted to pathogens. *Int. J. Immunopathol. Pharmacol.* 2004; 17:245. [PubMed: 15461858]
11. Demidova TN, Hamblin MR. Macrophage-targeted photodynamic therapy. *Int. J. Immunopathol. Pharmacol.* 2004; 17:117. [PubMed: 15171812]
12. Hamblin MR, Miller JL, Ortel B. Scavenger-receptor targeted photodynamic therapy. *Photochem. Photobiol.* 2000; 72:533. [PubMed: 11045726]
13. Murakami T, Yamada N. Modification of macrophage function and effects on atherosclerosis. *Curr. Op. Lipidol.* 1996; 7:320.
14. Kaisho T, Akira S. Critical roles of toll-like receptors in host defense. *Crit. Rev. Immunol.* 2000; 20:393. [PubMed: 11145217]



15. Kopp EB, Medzhitov R. The Toll-receptor family and control of innate immunity. *Curr. Opin. Immunol.* 1999; 11:13. [PubMed: 10047546]
16. Muzio M, Mantovani A. Toll-like receptors. *Microbes Infect.* 2000; 2:251. [PubMed: 10758401]
17. Ingalls RR, Heine H, Lien E, Yoshimura A, Golenbock D. Lipopolysaccharide recognition, CD14, and lipopolysaccharide receptors. *Infect. Dis. Clin. North Am.* 1999; 13:341. [PubMed: 10340170]
18. Brown GD, Taylor PR, Reid DM, Willment JA, Williams DL, Martinez-Pomares L, Wong SY, Gordon S. Dectin-1 is a major beta-glucan receptor on macrophages. *J. Exp. Med.* 2002; 196:407. [PubMed: 12163569]
19. Frantz S, Kobzik L, Kim YD, Fukazawa R, Medzhitov R, Lee RT, Kelly RA. Toll4 (TLR4) expression in cardiac myocytes in normal and failing myocardium. *J. Clin. Invest.* 1999; 104:271. [PubMed: 10430608]
20. Winston BW, Krein PM, Mowat C, Huang Y. Cytokine-induced macrophage differentiation: a tale of 2 genes. *Clin. Invest. Med.* 1999; 22:236. [PubMed: 10664866]
21. Takata K, Horiuchi S, Morino Y. Scavenger receptor-mediated recognition of maleylated albumin and its relation to subsequent endocytic degradation. *Biochim. Biophys. Acta.* 1989; 984:273. [PubMed: 2775777]
22. McHale AP, McHale L. Use of a tetrazolium based colorimetric assay in assessing photoradiation therapy in vitro. *Cancer Lett.* 1988; 41:315. [PubMed: 3409210]
23. Osterud B, Bjorklid E. Role of monocytes in atherogenesis. *Physiol. Rev.* 2003; 83:1069. [PubMed: 14506301]
24. Ashkenas J, Penman M, Vasile E, Acton S, Freeman M, Krieger M. Structures and high and low affinity ligand binding properties of murine type I and type II macrophage scavenger receptors. *J. Lipid Res.* 1993; 34:983. [PubMed: 8394868]
25. Krieger M. Molecular flypaper and atherosclerosis: structure of the macrophage scavenger receptor. *Trends Biochem. Sci.* 1992; 17:141. [PubMed: 1585457]
26. Haberland ME, Fogelman AM. Scavenger receptor-mediated recognition of maleyl bovine plasma albumin and the demaleylated protein in human monocyte macrophages. *Proc. Natl. Acad. Sci. USA.* 1985; 82:2693. [PubMed: 3857610]
27. Yamada Y, Doi T, Hamakubo T, Kodama T. Scavenger receptor family proteins: roles for atherosclerosis, host defence and disorders of the central nervous system. *Cell. Mol. Life Sci.* 1998; 54:628. [PubMed: 9711230]
28. Mukhopadhyay A, Mukhopadhyay B, Basu SK. Circumvention of multidrug resistance in neoplastic cells through scavenger receptor mediated drug delivery. *FEBS Lett.* 1995; 376:95. [PubMed: 8521976]
29. Barbour SE, Wong C, Rabah D, Kapur A, Carter AD. Mature macrophage cell lines exhibit variable responses to LPS. *Mol. Immunol.* 1998; 35:977. [PubMed: 9881693]
30. Frankenberger M, Ziegler-Heitbrock HW. LPS tolerance in monocytes/macrophages: three 3' cytosins are required in the DNA binding motif for detection of upregulated NF-kappa B p50 homodimers. *Immunobiology.* 1997; 198:81. [PubMed: 9442380]
31. Fujihara M, Wakamoto S, Ito T, Muroi M, Suzuki T, Ikeda H, Ikebuchi K. Lipopolysaccharide-triggered desensitization of TNF-alpha mRNA expression involves lack of phosphorylation of IkappaBalpha in a murine macrophage-like cell line, P388D1. *J. Leukoc. Biol.* 2000; 68:267. [PubMed: 10947072]
32. Victor VM, De la Fuente M. N-acetylcysteine improves in vitro the function of macrophages from mice with endotoxin-induced oxidative stress. *Free Radic. Res.* 2002; 36:33. [PubMed: 11999701]
33. Hunt DW, Jiang HJ, Levy JG, Chan AH. Sensitivity of activated murine peritoneal macrophages to photodynamic killing with benzoporphyrin derivative. *Photochem. Photobiol.* 1995; 61:417. [PubMed: 7740088]
34. Orlofsky A, Somogyi RD, Weiss LM, Prystowsky MB. The murine antiapoptotic protein A1 is induced in inflammatory macrophages and constitutively expressed in neutrophils. *J. Immunol.* 1999; 163:412. [PubMed: 10384143]
35. Kausalya S, Somogyi R, Orlofsky A, Prystowsky MB. Requirement of A1-a for bacillus Calmette-Guerin-mediated protection of macrophages against nitric oxide-induced apoptosis. *J. Immunol.* 2001; 166:4721. [PubMed: 11254733]

36. Van Lenten BJ, Fogelman AM, Seager J, Ribic E, Haberland ME, Edwards PA. Bacterial endotoxin selectively prevents the expression of scavenger-receptor activity on human monocyte-macrophages. *J. Immunol.* 1985; 134:3718. [PubMed: 2985693]
37. Fitzgerald ML, Moore KJ, Freeman MW, Reed GL. Lipopolysaccharide induces scavenger receptor A expression in mouse macrophages: a divergent response relative to human THP-1 monocyte/macrophages. *J. Immunol.* 2000; 164:2692. [PubMed: 10679110]
38. Geng YJ, Hansson GK. Interferon-gamma inhibits scavenger receptor expression and foam cell formation in human monocyte-derived macrophages. *J. Clin. Invest.* 1992; 89:1322. [PubMed: 1556191]
39. Grewal T, Priceputu E, Davignon J, Bernier L. Identification of a gamma-interferon-responsive element in the promoter of the human macrophage scavenger receptor A gene. *Arterioscler. Thromb. Vasc. Biol.* 2001; 21:825. [PubMed: 11348881]
40. Lougheed M, Steinbrecher UP. Mechanism of uptake of copper-oxidized low density lipoprotein in macrophages is dependent on its extent of oxidation. *J. Biol. Chem.* 1996; 271:11798. [PubMed: 8662601]
41. Marsche G, Zimmermann R, Horiuchi S, Tandon NN, Sattler W, Malle E. Class B scavenger receptors CD36 and SR-BI are receptors for hypochlorite-modified low density lipoprotein. *J. Biol. Chem.* 2003; 278:47562. [PubMed: 12968020]
42. Podrez EA, Febbraio M, Sheibani N, Schmitt D, Silverstein RL, Hajjar DP, Cohen PA, Frazier WA, Hoff HF, Hazen SL. Macrophage scavenger receptor CD36 is the major receptor for LDL modified by monocyte-generated reactive nitrogen species. *J. Clin. Invest.* 2000; 105:1095. [PubMed: 10772654]
43. Podrez EA, Poliakov E, Shen Z, Zhang R, Deng Y, Sun M, Finton PJ, Shan L, Gugiu B, Fox PL, Hoff HF, Salomon RG, Hazen SL. Identification of a novel family of oxidized phospholipids that serve as ligands for the macrophage scavenger receptor CD36. *J. Biol. Chem.* 2002; 277:38503. [PubMed: 12105195]
44. Brown MS, Basu SK, Falck JR, Ho YK, Goldstein JL. The scavenger cell pathway for lipoprotein degradation: specificity of the binding site that mediates the uptake of negatively-charged LDL by macrophages. *J. Supramol. Struct.* 1980; 13:67. [PubMed: 6255257]

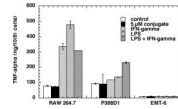


**Fig. 1.**

TNF $\alpha$  secretion by cells in response to conjugate, IFN $\gamma$  and/or LPS. TNF $\alpha$  secreted into the culture medium was measured with the cytometric bead array as described after 24 or 48-hour incubation of the cells with conjugate (2- $\mu$ M), IFN $\gamma$  (100 U/mL) and/or LPS (100 ng/mL). Values are expressed as ng/10<sup>6</sup> cells and values are means of six experiments with error bars representing SEM. \* = P < 0.05; \*\* = P < 0.01; \*\*\* = P < 0.001 versus control cells.

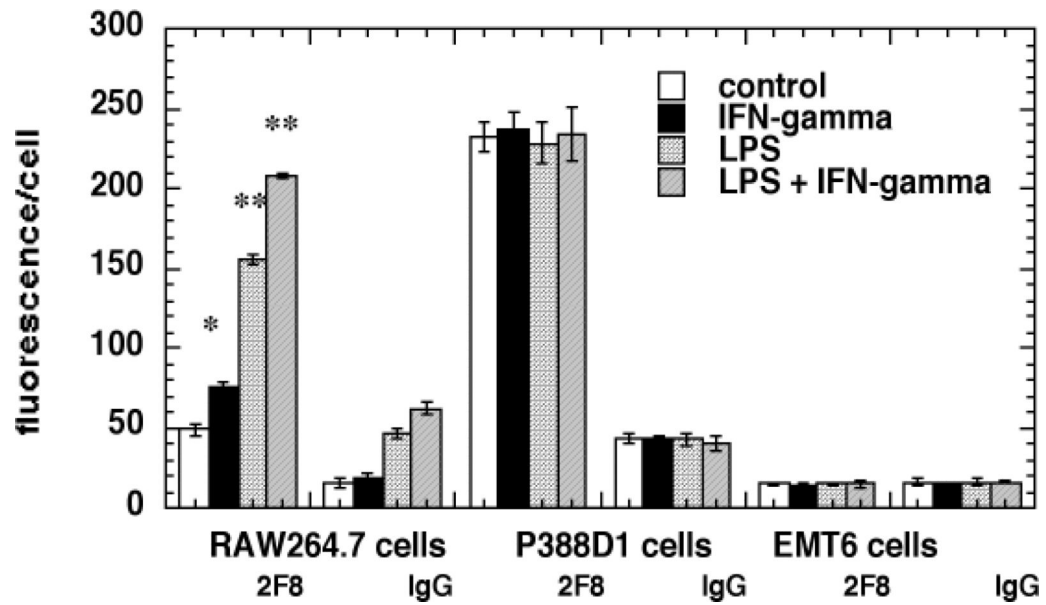


**Fig. 2.** Scavenger receptor class A expression on cells. Cells were removed with an enzyme-free dissociation reagent, washed and incubated with FITC labeled anti-SRA antibody 2F8 or isotype-matched control IgG 2b (20 nM) for 2-hours at 4°C. Cell associated fluorescence was then analyzed by flow cytometry. Values are means of six experiments and bars are SEM. \* =  $P < 0.05$ ; \*\* =  $P < 0.01$ ; \*\*\* =  $P < 0.001$  versus control cells.

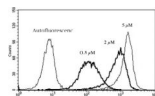


**Fig. 3.** Use of flow cytometry to quantify PS uptake by unstimulated RAW264.7 cells incubated for 24-hours with increasing concentrations of BSA-ce6-mal. For each condition, the mean fluorescence intensity of 10,000 gated singlet cells from the histogram statistics was recorded.



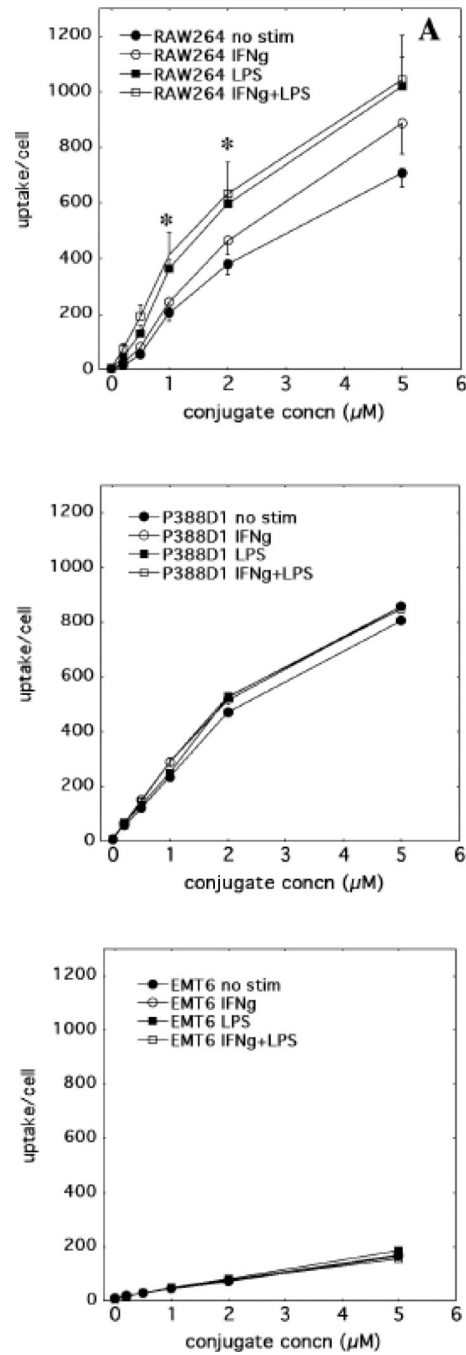


**Fig. 4.** Cell uptake with increasing conjugate concentrations. Cells were activated as described and incubated with increasing conjugate concentrations and analyzed by flow cytometry. Values are means of three experiments and error bars are SEM. \* =  $P < 0.05$ ; versus unstimulated cells.

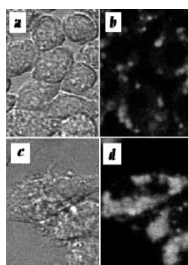


**Fig. 5.** Confocal photomicrographs. Phase contrast (a and c) and fluorescence images (b and d) of RAW264.7 cells incubated with BSA-cc6-mal . a and b; Unstimulated RAW264.7 cells; c and d; RAW264.7 cells treated with IFN $\gamma$  + LPS.

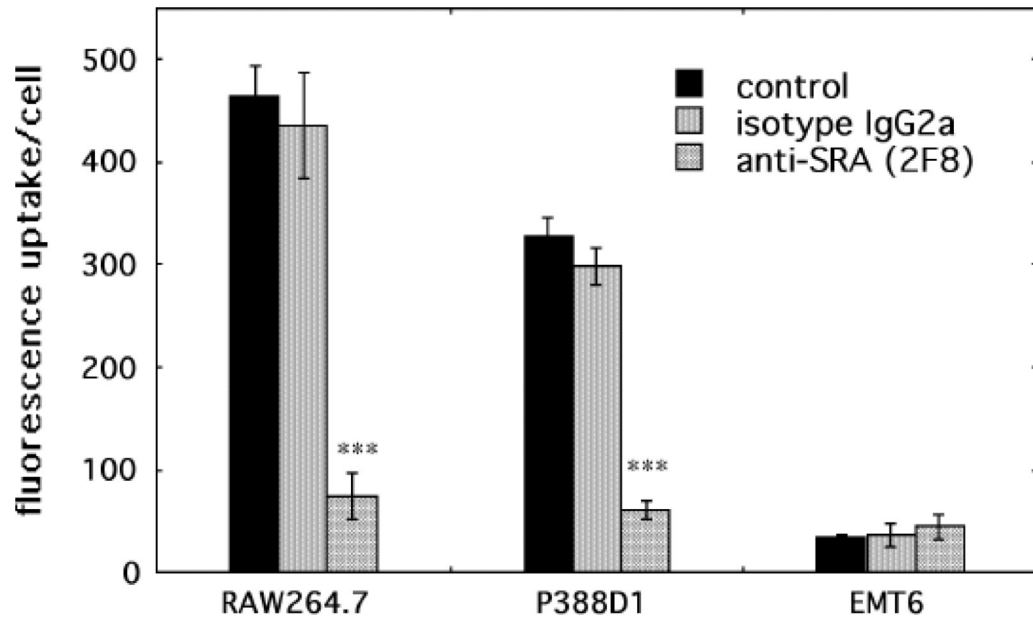


**Fig. 6.** Effect of preincubation with anti-SRA antibody or control IgG on uptake of conjugate by cells. Cells were incubated with unlabeled 2F8 or IgG 2b at 20 nM for 1 hour at 37°C followed by addition of 2  $\mu$ M conjugate for 24-hours and analyzed by flow cytometry. Values are means of three experiments and bars are SEM. \*\*\* =  $P < 0.001$  versus control

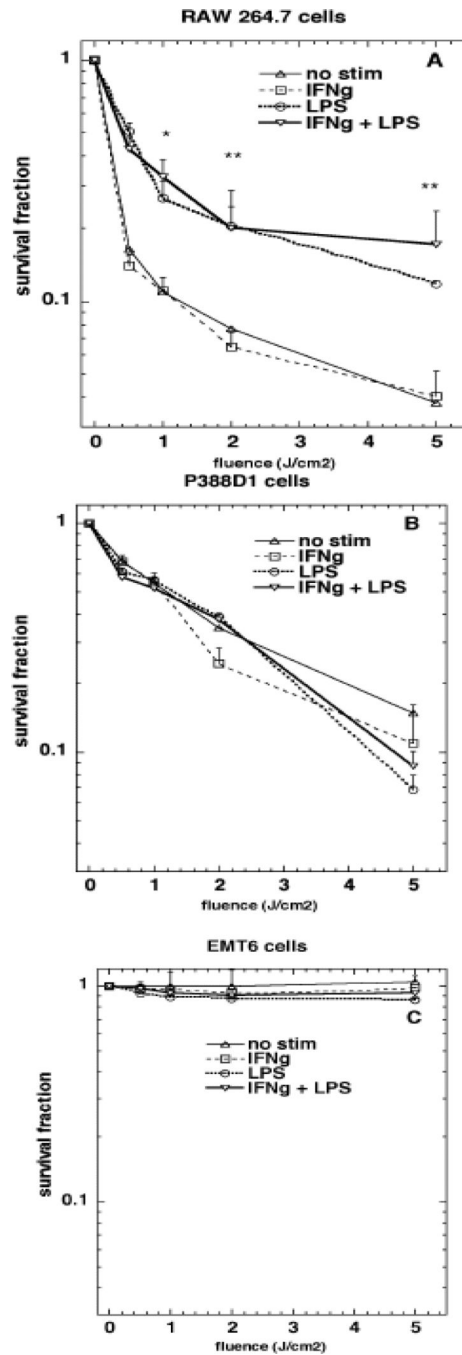


**Fig. 7.** Photodynamic therapy. Cells were incubated with conjugate for 24 hours and illuminated with 670-nm light at a fluence rate of 50 mW/cm<sup>2</sup> and survival fractions were calculated with respect to nonilluminated cells by the MTT assay. Values are means of 15 wells and bars are SEM. \* = P < 0.05; \*\* = P < 0.01; versus unstimulated cells.

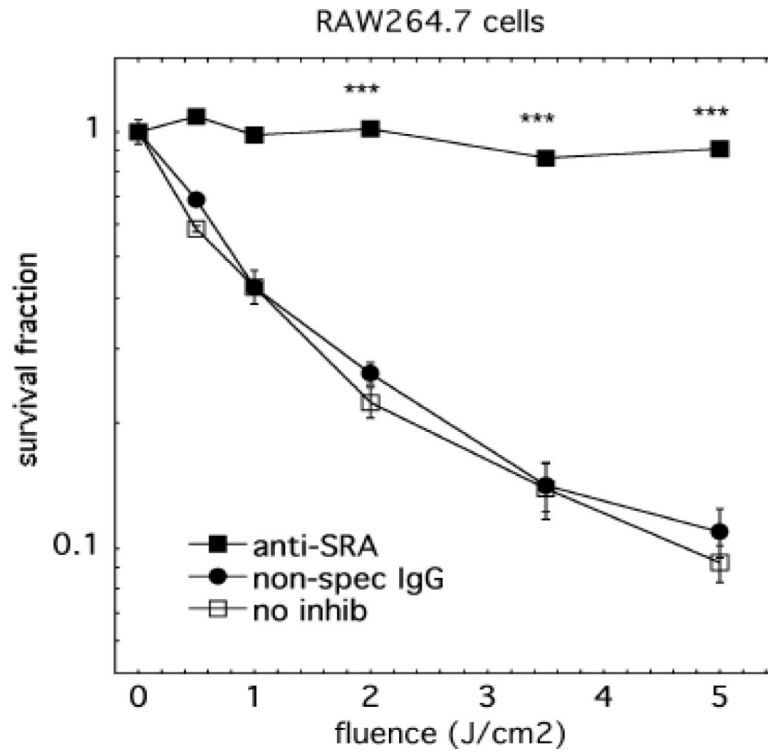


**Fig. 8.** Protection from killing by anti-SRA 2F8. Raw264.7 cells were preincubated with 2F8, control IgG2b or nothing before having conjugates added for 24 hours and then being illuminated. Values are means of 12 wells and bars are SE. \*\*\* =  $P < 0.001$  versus no inhibition.